ELSEVIER

International Journal of Pharmaceutics 154 (1997) 217–227

international journal of pharmaceutics

# Comparison of permeability data from traditional diffusion cells and ATR-FTIR spectroscopy. Part II. Determination of diffusional pathlengths in synthetic membranes and human stratum corneum

Mark A. Pellett [a], Adam C. Watkinson [b,*], Jonathan Hadgraft [a], Keith R. Brain [a,b]

[a] *The Welsh School of Pharmacy, University of Wales, Cardiff, CF1 3XF, UK*
[b] *An-eX, Redwood Building, King Edward VII Avenue, Cardiff, CF1 3XF, UK*

Received 6 March 1997; received in revised form 29 April 1997; accepted 6 May 1997

**Abstract**

In this study, the morphological structure of the inner and outer regions of human stratum corneum (SC) were investigated using Attenuated Total Reflectance Fourier Transform Infra-Red (ATR-FTIR) spectroscopy. Furthermore, diffusional pathlengths in silicone membranes and human SC were determined using ATR-FTIR spectroscopic data and regular skin diffusion cell data. SC membranes were fully hydrated throughout the experiments. It was shown that diffusion coefficients for a model permeant, 4-cyanophenol (CP), were lower in the more compact regions of the inner layers of the SC when compared to diffusion coefficients in the outer layers. Partition coefficients between SC and aqueous vehicles were higher in the outer layers than the inner layers. These data demonstrate a 4-fold lower permeability of skin to CP in the inner layers relative to the outer layers of the SC. The combination of diffusion cell data and ATR-FTIR spectroscopic data was also used to determine diffusional pathlengths across synthetic silicone membranes and human SC. In all cases, the pathlengths were similar to the thickness of the membranes. For SC, this appears to contrast the commonly held theory that diffusion occurs via a tortuous route within the intercellular lipids, and may therefore imply a transcellular route. Alternatively, the calculated pathlengths may be a reflection of the total length of rate limiting steps in the diffusional process rather than overall diffusional distance. This implies that lateral molecular diffusion within the head groups or lipid tails (depending on the lipophilicity of the permeant) of the lipid bilayers may be a relatively rapid process. These results have demonstrated that the previously observed morphological differences between the inner and outer regions of the SC are reflected in variations in permeability, and that the diffusional route through fully hydrated human SC may indeed be via a direct pathway. © 1997 Elsevier Science B.V.

*Keywords:* Fourier transform infrared spectroscopy; Attenuated total reflectance; Diffusional pathlength; Silicone membranes; Human stratum corneum; Morphology

* Corresponding author. Tel.: +44 1222 874952; fax: +44 1222 874952; e-mail acw@an-ex.co.uk


*PII* S0378-5173(97)00143-9

## 1. Introduction

The theory and application of Attenuated Total Reflectance Fourier Transform Infra-Red (ATR-FTIR) spectroscopy for the assessment of diffusion through membranes have been described elsewhere (Farinas et al., 1994; Wurster et al., 1993; Harrick, 1967). Data from diffusion cells can be used to calculate diffusion coefficients, by use of the lag time $t_{lag}$ (Eq. (2)). However, the reliability of this method has recently been questioned (Potts and Guy, 1994) as it relies heavily on the attainment of steady-state diffusion. One of the key advantages that the ATR-FTIR technique has over the use of diffusion cells is that it can be used to deconvolute the permeability coefficient, $k_p$, into its individual components (the diffusion coefficient, $D$, the membrane/vehicle partition coefficient, $K$, and diffusional pathlength, $h$ (1)) without the need to attain or define steady-state diffusion.

$$k_p = \frac{KD}{h} \quad (1)$$

$$t_{lag} = \frac{h^2}{6D} \quad (2)$$

Using this approach ATR-FTIR spectroscopy has been used to separate the enhancing effects of Transcutol® and Azone® on flux through human stratum corneum (SC) (Harrison et al., 1996), and also to investigate vehicle effects on permeation across synthetic membranes (Watkinson et al., 1995). In that work the effects of enhancers and vehicles on the diffusion and partition coefficients were individually evaluated.

However, measurement of the partition coefficients only involved semiquantitative comparison of plateau levels (where plateau levels reflected the partitioning behaviour but did not allow calculation of an absolute partition coefficient). This issue of quantitation has been addressed using synthetic membranes and calibration of the ATR-FTIR system so that calculation of absolute membrane/vehicle partition coefficients and subsequent derivation of permeability coefficients was possible (Pellett et al., 1997). The correlation between the permeability coefficients derived from this ATR-FTIR study and those determined using diffusion cells was high.

In the present study the ATR-FTIR system was calibrated for use with an alternative membrane (isolated human SC) so that absolute permeability coefficients in this material could be calculated and compared to those obtained using diffusion cells. The ATR-FTIR system was also used to investigate SC morphology and the diffusional pathlength in both SC and synthetic membranes. Isolated SC is known to be a heterogeneous structure composed of corneocytes, which are packed with keratin and surrounded by an intercellular matrix of highly ordered lipid bilayers (Elias, 1991). Diffusion through the SC is thought to occur primarily through regions of intercellular lipid around the cells and thus the diffusional pathlength is thought to be greater than the membrane thickness. It is also considered that the lipid layers which are closer to the epidermis offer more resistance to permeation than those at the surface. Therefore, diffusion and partition coefficients may be predicted (Watkinson et al., 1992) to be different in the superficial layers of the SC (outer layers) than in those adjacent to the viable epidermis (inner layers). ATR-FTIR spectroscopy provides a limited depth of penetration ($\sim 2-3$ μm) of the IR beam into the membrane. It is therefore theoretically possible to probe the microstructure of the outer and inner regions of the SC by evaluation of any differences between data obtained by placing the outer and inner surfaces of isolated SC on the ATR crystal.

## 2. Materials and methods

### 2.1. Materials

4-Cyanophenol (95%) and bovine trypsin were purchased from Aldrich (Dorset, UK); methanol, chloroform and hexane (all HPLC grade) from Fisher (Loughborough, UK); acetonitrile (HPLC grade) from Rathburn (Walkerburn, UK). Samco silicone membranes (St. Albans, Herts, UK) had a measured thickness of either 275 or 770 μm (micrometer, Wright and Moore). Sil-Tec silicone membrane (Technical Products, USA) had a mea-

sured thickness of 90 μm. Tritiated water (5.0 mCi $ml^{-1}$) was obtained from Amersham International and HiSafe scintillation fluid from Wallac. All materials were used as received unless otherwise indicated. Full thickness abdominal human skin was obtained after cosmetic surgery at a local hospital and stored frozen at −20°C until required.

### 2.2. Preparation of isolated human stratum corneum

After thawing overnight and removal of adipose tissue by blunt dissection, the skin was immersed in water at 60°C for 1 min. It was then pinned to a cork board and the epidermis carefully peeled away from the dermis. The viable tissue was removed by soaking the membrane in a phosphate buffered saline solution containing 0.0001% trypsin for 24 h at 37°C. The SC was quickly dipped in hexane before placing in tepid water and floating the membrane onto filter paper supports. It was allowed to air dry before storing at −20°C until required.

### 2.3. Diffusion cell studies

The diffusion of saturated solutions of cyanophenol (in the presence of excess solid) across silicone membranes of 90, 275 and 770 μm thickness and across isolated SC were monitored using diffusion cells. To counteract any change in barrier function, due to progressive hydration during the experiment, the silicone membranes were pre-soaked in water for 48 h before use. SC (supported on filter paper) and silicone membranes were mounted in diffusion cells and allowed to equilibrate for 1 h before application of the donor phase (1 ml of a saturated solution of cyanophenol). Previous experiments (Pellett et al., 1995, and unpublished data) have shown that these procedures ensure complete hydration of each type of membrane.

Diffusion cell experiments (where cyanophenol was the permeant) were performed at ambient temperature (~23°C), as elevated temperatures could not be applied to the ATR crystal. Phosphate buffered saline (pH 7.4) was used as the receptor phase for experiments with SC, and water for silicone membranes. All receptor phases were degassed by vacuum filtration through a 0.45 μm cellulose nitrate membrane filter. Diffusional surface areas were ~1 $cm^2$ and receptor volumes ~2.5 ml. Magnetic followers were added to each receptor compartment and cells were placed on a magnetic stirring bed. Samples (400 μl) were taken at pre-determined time points and replaced with an equal volume of receptor phase. Permeability coefficients were determined from the diffusion profiles obtained using the $P_1P_2$ method (Watkinson et al., 1994).

Tritiated water permeability across three different skin preparations (SC and epidermal membranes as prepared above and full thickness skin) was determined at 37°C using skin diffusion cells. Skin samples were mounted in the diffusion cells and treated with 500 μl of tritiated water (2 μCi $ml^{-1}$) and permeation of the labelled material monitored by sampling the receptor phase (pH 7.4 phosphate buffered saline) over a 10-h period. Five replicates were conducted for each skin preparation. Samples were assessed for radioactivity using a Wallac 1409 scintillation counter after addition to 3 ml of scintillation fluid.

### 2.4. ATR-FTIR spectroscopy studies

The general experimental methodology has been described in detail in a previous publication (Pellett et al., 1997) and only minor amendments were necessary to adapt the system for use with human SC. Optimal signal strength is obtained when the entire surface of the ATR crystal is covered by the test membrane. A full-length donor compartment (exposed surface area 4.2 $cm^2$) was therefore used for silicone membranes. However, as a consequence of practical limitations in preparation and positioning, it was found necessary to use a shorter donor compartment for SC membranes (exposed surface area 2.1 $cm^2$).

The prepared SC was allowed to thaw completely before cutting into strips. After soaking in water for ~1 h to remove the filter paper, the SC membranes were floated onto a Teflon® mesh, blotted dry with paper tissue and placed on the ATR crystal. Diffusion into SC membranes was

separately examined with either the outer or inner surface in contact with the ATR crystal. Pre-soaked silicone membranes (90, 275 and 770 μm) were blotted dry with paper tissue and placed on the crystal. Sufficient volumes of saturated aqueous solutions of cyanophenol (with excess solid present) to maintain constant thermodynamic activity were added to each donor compartment (1 ml for biological and 4 ml for synthetic membranes). Ten FTIR scans were taken at each time point for the silicone membranes and five scans at each time point for the SC membranes, and diffusion coefficients and plateau levels were determined from the resultant permeation profiles using the cyano (CN) peak area of cyanophenol. Values for $D$, or $D/h^2$, and plateau levels were determined as described previously (Pellett et al., 1997).

Due to differences in the degree of contact between different SC samples and the ATR crystal, all plateau levels ($A_0$) were normalised to the intensity (I) of the Amide II peak of SC at around 1550 $cm^{-1}$ (Knutson et al., 1985).

$$A_{0(\text{Normalised})} = \frac{A_0}{I} \quad (3)$$

Fig. 1 shows that the Amide II stretch frequency is distinct from the stretching frequencies of the other materials used in this study.

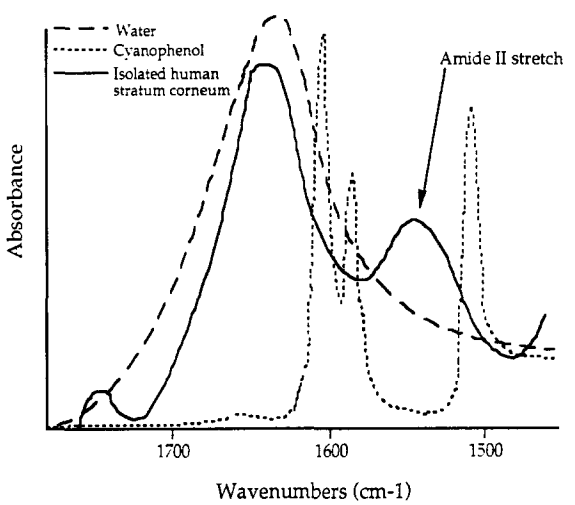


Fig. 1. FTIR spectra of water, 4-cyanophenol and human SC.

### 2.5. Calibration of the ATR crystal

Sections of SC ( ~ 4 cm × 2 cm) were prepared as described above and the weight ( ~ 15 mg) of each sample was measured. After soaking overnight in ~ 30 ml of aqueous solutions of cyanophenol of concentrations ranging from 3 to 13.5 mg $ml^{-1}$, the SC was floated back onto a Teflon mesh, blotted dry with tissue, placed on the ATR crystal, and the CN peak area was determined and normalised to the intensity of the Amide II stretch frequency as described above.

Cyanophenol was extracted from the SC by placing it in 3 ml of a 50/50 mixture of chloroform and methanol. After 16 h, 2 ml (67%) of the chloroform/methanol mixture was removed and evaporated to dryness. The residue was dissolved in 1 ml of methanol and assayed for cyanophenol by HPLC using the conditions described previously. Complete extraction was confirmed after a second extraction using the same procedure resulted in undetectable levels of cyanophenol.

## 3. Results and discussion

### 3.1. Diffusion cell studies

Fig. 2a shows the diffusion profiles of cyanophenol across the 275 and 770 μm silicone membranes, both of which had been soaked in water prior to the experiment. Fig. 2b shows the diffusion of cyanophenol across the 90-μm silicone membrane (also soaked in water) and isolated human SC.

Sink conditions were maintained throughout all three experiments with ~ 0.3 mg $ml^{-1}$ in the receptor phase at the final time point for the SC and SilTec experiments, and ~ 0.06 and ~ 0.08 mg $ml^{-1}$ for 770 μm and 275-μm silicone membrane experiments, respectively (the aqueous saturated solubility of cyanophenol was 15.1 mg $ml^{-1}$). Permeability coefficients were calculated using the $P_1P_2$ method (Watkinson et al., 1994) and are shown in Table 1. In this experiment, it appears that Sil-Tec 90-μm membranes had a similar permeability to that of human SC. Human SC was approximately four times more permeable

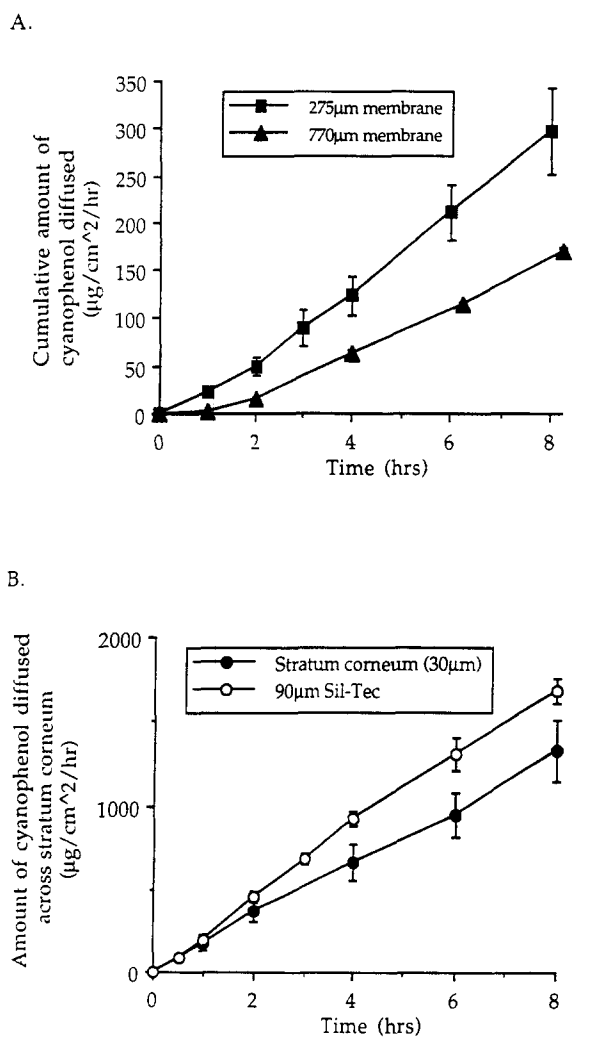


Fig. 2. Cumulative amount of cyanophenol that diffused across 275 and 770 μm silicone membranes (a) and, isolated human stratum corneum (30 μm) and 90 μm Sil-Tec membranes (b).

than silicone membranes of 275 μm thickness, and seven times more permeable than silicone membranes of 770 μm thickness.

The 770 and 275 μm membranes were obtained from the same manufacturer and are nominally described as the same polymer. Hence, one would have expected a 2.8 fold difference (770/275) in the permeability coefficients of these membranes but only a 1.8 fold difference (2.76/1.52) was observed. This anomaly was attributed to manufacturer variations with silicone consistency prior to casting the membranes (see Table 2, and below).

### 3.2. ATR-FTIR studies using silicone membranes

Values for diffusion coefficients and plateau levels for cyanophenol in the three thicknesses of silicone membrane are shown in Table 2 together with partition coefficients calculated using a previously obtained calibration plot ($A_0 = -3.23 \times 10^{-2} + 6.59 \times 10^{-4}.C_0$, where $A_0$ is the plateau level and $C_0$ the concentration (μg $ml^{-1}$) of cyanophenol in the membrane (Pellett et al., 1997)). The use of this calibration graph makes the assumption that any differences in the optical properties of the silicone membranes are negligible. Table 2 also contains permeability coefficients calculated from the appropriate values of $D$, $h$, and $K$. In general, there is good agreement between the permeability coefficients calculated from the ATR-FTIR spectroscopic data (Table 2) and those calculated from the diffusion cell data (Table 1).

Table 1
Flux and permeability coefficients for the diffusion of cyanophenol across silicone membranes and human stratum corneum (from diffusion cells)

| Membrane | Flux (μg $cm^{-2}$ $h^{-1}$) | Permeability coefficient × $10^{-3}$ (cm $h^{-1}$) |
|---|---|---|
| Silicone membrane (770 μm) | 23.0 ± 10.3 | 1.52 ± 0.68 |
| Silicone membrane (275 μm) | 41.7 ± 5.40[a] | 2.76 ± 0.36[a] |
| Silicone membrane (90 μm) | 221 ± 12.4 | 14.6 ± 0.82 |
| Stratum corneum | 157 ± 21.1 | 10.4 ± 1.4 |

Mean values ± S.E., ($n \geq 24$).
[a] Data from Pellett et al. (1997).

Table 2
Diffusion coefficients ($D$), plateau levels, partition coefficients ($K$) and resultant permeability coefficients ($k_p$) for cyanophenol in silicone membranes (from ATR-FTIR studies)

| Thickness of membranes (μm) | $D$ ($cm^2\ h^{-1}$) | Plateau level | $K$ | $k_p$ ($cm\ h^{-1}$) $\times 10^{-3}$ |
|---|---|---|---|---|
| 770 μm | $9.23 \pm 0.43$ | $1.72 \pm 0.08$ | 0.176 | 2.11 |
| 275 μm | $6.34 \pm 0.57$[a] | $1.31 \pm 0.04$[a] | 0.132 | 3.04 |
| 90 μm | $9.19 \pm 0.61$ | $1.42 \pm 0.16$ | 0.146 | 14.9 |

Mean ± S.E., ($n = 3$).
[a] Data from Pellett et al. (1997).

### 3.3. Investigation of stratum corneum morphology using ATR-FTIR spectroscopy

Isolated SC is a heterogeneous structure through which diffusion is thought to occur primarily via tortuous lipoidal pathways. It is also considered that the lipid layers which are closer to the viable epidermis offer more resistance to permeation than those at the surface. Therefore, diffusion and partition coefficients may be predicted (Watkinson et al., 1992) to be different in the superficial layers of the SC (outer layers) than in those adjacent to the viable epidermis (inner layers). ATR-FTIR spectroscopy provides a limited depth of penetration ($\sim 2$–$3$ μm) of the IR beam into the membrane. It is therefore theoretically possible to probe the microstructure of the outer and inner regions of the SC by evaluation of any differences between data obtained by placing the outer and inner surfaces of isolated SC on the ATR crystal.

Sections of SC were equilibrated with aqueous solutions of varying concentration of cyanophenol. After removal from the aqueous solutions, the sections of SC were blotted with tissue paper and then placed on the ATR crystal and the resultant CN peak area was measured. Fig. 3 shows data collected with both the inner and outer layers of the SC in contact with the ATR crystal and it is clear that there is little difference between the two sets of data. The similarity between these data sets was initially surprising, considering the known heterogeneity of SC, i.e. one might expect that the outer layers, being less tightly packed, would take up more permeant than the more tightly packed inner layers. However, the experimental procedure involved removing excess solution from the membrane surfaces by blotting with tissue before application to the ATR crystal. This procedure may have inadvertently removed some of the permeant from the less tightly packed areas of the outer surface of the SC and hence reduced the CN peak areas obtained in the calibration plot.

Additionally, the less structurally dense region of the outer layers of the SC may also be optically less dense than the inner layers. This may have led to lower penetration of the IR beam into the outer layers of the SC (the actual difference being dependent on the difference in refractive index of the inner and outer SC) than into the inner layers. Such an effect (as well as the possibility of removal of material by wiping) would reduce the signal from the outer layers relative to the inner

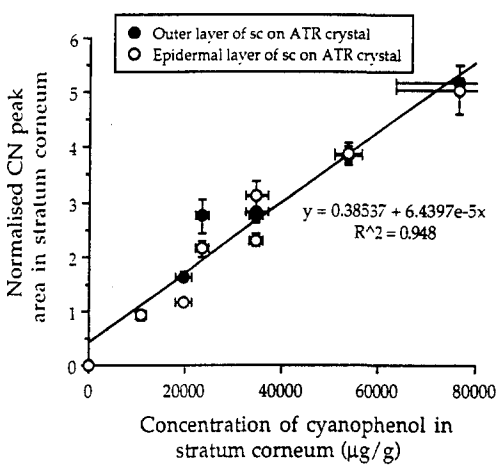


Fig. 3. Plot of cyanophenol uptake by the inner and outer layers of stratum corneum as measured by ATR-FTIR spectroscopy (Mean ± S.E., $n = 3$). Linear regression performed using data for inner layer only (see text).

Table 3
Values for $D/h^2$, normalised plateau levels, and partition coefficients as determined for the two sides of the isolated preparations of stratum corneum on the ATR crystal

| Side of stratum corneum adjacent to ATR crystal | $D/h^2$ ($h^{-1}$) | Normalised plateau level | $K$ |
|---|---|---|---|
| Outer | $0.703 \pm 0.079$ | $4.83 \pm 0.63$ | $4.96 \pm 0.65$ |
| Inner | $1.660 \pm 0.288$ | $2.84 \pm 0.21$ | $2.92 \pm 0.21$ |

Mean $\pm$ S.E., ($n = 4$).
In a 2-tailed $t$-test for $D/h^2$ $P = 0.049$: for normalised plateau levels $P = 0.058$.

layers. However, this effect was modelled (see Appendix I) and shown to be an unlikely explanation. Therefore, the former of the two possible reasons outlined above may explain why the two data sets in Fig. 3 are not different as might have been expected from a consideration of the morphology of the SC.

To investigate this phenomenon further, diffusion experiments were conducted by placing SC samples on the ATR crystal with firstly the outer side of the SC in contact with the crystal and secondly the inner side of the SC in contact with the crystal. This approach, therefore, eliminates any error introduced into the measurements made as described above by the wiping procedure. Any difference between the two plateau levels will be due to possible differences in beam penetration depth and not inadvertent removal of material by the wiping procedure. Hence, if a difference is observed, it is likely to be lower than the real value due to this difference in penetration depth. As can be seen from Table 3, the plateau level in the outer SC was approximately twice that measured in the inner SC. Thus, we can conclude that the outer region of SC contains at least twice as much permeant as the inner region, and that this is likely to be a direct result of the less cohesive nature of the SC structure.

Unlike the silicone membranes, definitive values for the diffusion coefficients of cyanophenol in SC could not be determined because the diffusional pathlengths were unknown. Therefore, Table 3 quotes values for $D/h^2$ for the two sides of SC (inner and outer) placed on the ATR crystal.

When the outer side of the SC was placed on the surface of the ATR crystal, it was assumed that the intercellular lipids and corneocytes adjacent to the crystal surface presented lower resistance to diffusing permeants than the lipids and corneocytes in the inner layers. As the infrared beam of the ATR-FTIR spectrometer penetrated perhaps 2–3 μm into the membrane, we suggest that cyanophenol would be detected before it reached the more permeable layers next to the ATR crystal. Hence, the $D/h^2$ values measured whilst the outer SC was in contact with the crystal may well be a reflection of the $D/h^2$ values of the less permeable deeper layers rather than the outer layers themselves. In the case where the inner SC is in contact with the crystal the same principle may apply and the detection of cyanophenol will be dependent more on the layers that are 2–3 μm above the crystal surface than those actually resting on it.

If these assumptions are correct, then the value of $D/h^2$ obtained with the outer SC in contact with the membrane will reflect the value in the deeper regions and the value of $D/h^2$ obtained with the inner region in contact with the crystal will contain a contribution that reflects the value in the outer regions. As a result, values for $D/h^2$ were expected to be greater when the inner side of the SC was placed on the crystal than when the outer side was on the crystal. Table 3 shows values for $D/h^2$ for the two experiments involving the SC, and as predicted, there was a 2.4-fold greater value of $D/h^2$ for cyanophenol in SC when the inner side was on the crystal than when the outer side was on the crystal. As the diffusional pathlength is likely to be similar, irrespective of which side is placed on the ATR crystal, it can be confirmed that the SC is not a homogenous membrane (i.e. it is not a uniform distribution of corneocytes in a matrix of lipids) and the diffu-

Table 4
Calculation of diffusional pathlengths in silicone membranes and stratum corneum

| Membrane | $(KD/h^2)_{ATR\text{-}FTIR}$ ($h^{-1}$) | $(KD/h)_{Cells} \times 10^{-3}$ (cm $h^{-1}$) | $h$ (μm) |
|---|---|---|---|
| Silicone (770 μm) | 0.011 ± 0.001 | 1.52 ± 0.68 | 559 ± 27 |
| Silicone (275 μm) | 0.11 ± 0.01 | 2.76 ± 0.36 | 254 ± 22 |
| Silicone (90 μm) | 1.34 ± 0.10 | 14.6 ± 0.8 | 89 ± 6 |
| SC outer | 3.49 ± 0.39 | 10.4 ± 1.4 | 31 ± 4 |
| SC inner | 4.86 ± 0.84 | 10.4 ± 1.4 | 23 ± 4 |

Mean values ± S.E.

sional resistance is greater in the inner layers than the outer layers. This result is in keeping with that gained above for the relative partitioning behaviour of the inner and outer SC. An approximate idea of the overall difference in permeability of the inner and outer SC can be gained by ratioing the product of the relevant partition and diffusion coefficients. Calculation of the permeability of the outer layers of the SC relative to the inner layers yields a value of 4.0 ($4.83 \times 1.66/0.703 \times 2.84$) which compares favourably with the value of 2.9 predicted previously using a different method (Watkinson et al., 1992).

The 4-fold difference in permeability between the two sides of the SC implies greater partitioning of cyanophenol into the outer layers of the SC than into the layers closer to the epidermis. It is widely acknowledged that the cohesion of the cells of the SC increases as the tissue is penetrated (Watkinson et al., 1992). Hence, the observed difference in the degree of partitioning of permeant into the outer and epidermal sides of SC is probably a result of this structural gradient within the tissue, i.e. the corneocytes and intercellular lipids in the inner layers are more tightly packed and so there is less space for the cyanophenol to reside.

### *3.4. Comparison of in-vitro ATR-FTIR derived permeability data with ATR-FTIR in-vivo data*

A recent in-vivo study measured the permeation of cyanophenol from a saturated aqueous solution through human stratum corneum using ATR-FTIR spectroscopy (Pirot et al., 1997). This study predicted the value of the permeability coefficient and steady-state flux to be $3.7 \times 10^{-3}$ cm $h^{-1}$ and 85.7 μg $cm^{-2}$ $h^{-1}$, respectively. These predictions were based on an assumed diffusional pathlength of 15 μm which, if applied to the in-vitro ATR-FTIR results gained in the present work (Table 3), gives values for permeability and flux of $7.7 \times 10^{-3}$ cm $h^{-1}$ and 116 μg $cm^{-2}$ $h^{-1}$ respectively (using the averaged data for the inner and outer SC). Given the known variability of the permeability of skin, the agreement between these in-vivo ATR-FTIR data sets is extremely good.

### *3.5. Calculation of diffusional pathlength in silicone membranes and stratum corneum*

Table 1 contains the permeability coefficients ($k_p = KD/h$) of cyanophenol calculated from the diffusion cell experiments for each of the membranes examined. Calibration of the ATR-FTIR spectrometer and subsequent determination of partition coefficients from the plateau levels, allowed calculation of the composite parameter $(KD/h^2)_{ATR\text{-}FTIR}$ for the silicone membranes and SC (Tables 2 and 3). This differs from the permeability coefficient obtained from the diffusion cell data by a factor of $1/h$ (Eq. (4)).

$$\left(\frac{KD}{h^2}\right)_{ATR-FTIR} = \left(\frac{KD}{h}\right)_{Cells} \frac{1}{h} \quad (4)$$

Hence, by using regular diffusion cell data to calculate the permeability coefficient, $(KD/h)_{Cells}$, ATR-FTIR spectroscopy to find $D/h^2$ and determination of the partition coefficient ($K$), it was possible to calculate the diffusional pathlength ($h$) (Table 4). The correlation between experimental and measured values for these pathlengths appeared to increase as the membrane thickness reduced. Although the reasons for this phe-

nomenon are unknown, it is clear that, for the 90 μm membrane, the agreement was extremely good (99.7%). As it is very likely that the thickness of these membranes approximates to the diffusional pathlength within them, it was feasible that this method of prediction could be exploited to produce respectable estimates of pathlengths for relatively thin membranes. Similar calculations to those performed for the silicone membranes were, therefore, conducted using SC which are also shown in Table 4.

The experimental values for diffusional pathlength across SC (Table 4) are about 23 and 31 μm as calculated using the ATR-FTIR data (in conjunction with the diffusion cell data) for the inner and outer regions of the SC, respectively. At first sight, these results appear to contradict the common view that the route of diffusion through SC is tortuous with a pathlength of $\sim 300$–$900$ μm (Potts and Francoeur, 1991; Albery and Hadgraft, 1979) and suggests that a direct route across the swollen corneocytes may exist (Fig. 4). Alternatively, as the apparent pathlength is a reflection of total length of rate limiting steps in a diffusional process rather than overall diffusional distance, they may imply that, in fully hydrated SC, molecular lateral diffusion within lipid bilayers is a relatively rapid process (Fig. 4).

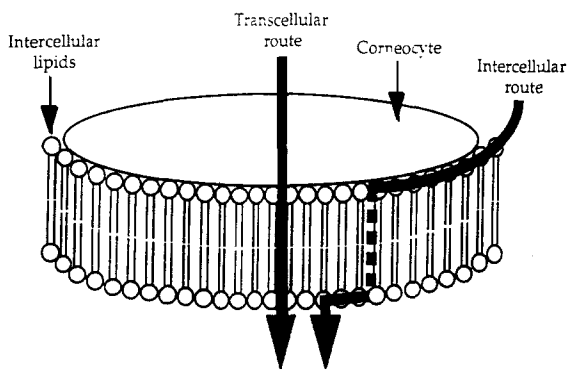


Fig. 4. Simplified diagram of the two theories relating the calculated pathlengths to SC: transcellular route across swollen corneocytes; intercellular route (for a hydrophilic compound shown in the diagram), where rapid lateral diffusion within polar lipid head groups occurs, and the rate limiting steps are considered to be transport across the lipid tails.

The diffusional pathlength for hydrophilic permeants may be sensitive to the degree of SC hydration. Water appears to enhance permeation (Roberts and Walker, 1993) but does not affect the repeat distance of the lipid bilayers (Bouwstra et al., 1991), but on full hydration, pools of water can be identified within the lamellar regions of the SC (van Hal et al., 1996). Hence, it is clear that water does penetrate these regions of the SC and it is therefore not unreasonable that its presence may produce a change in diffusional pathlength by one of the mechanisms outlined above. This has possible implications for the design and interpretation of in-vitro measurements that utilise aqueous receptor phases. Furthermore, it should also be noted that the use of aqueous donor phases (either in vitro or in vivo) may lead to morphological changes in the SC which may be responsible for the known enhancing effect of water.

Because the measured pathlength was small, and approximately the same order of magnitude as the SC thickness, it was feasible that the membrane had been damaged during the preparation process. To eliminate this possibility the permeation of tritiated water across SC was compared with that across epidermal membranes and full thickness skin. Permeability coefficients calculated from the resultant permeation profiles ($n = 5$ for each skin preparation) were $1.21 \times 10^{-3}$, $1.34 \times 10^{-3}$ and $1.30 \times 10^{-3}$ cm $h^{-1}$ for SC, epidermal membranes and full thickness skin respectively. Therefore, it can be assumed that the integrity of the skin was not compromised by the preparation procedures used to isolate SC. Hence, it is unlikely that the relatively short pathlengths obtained in this work can be explained by such a phenomena.

## 4. Conclusions

ATR-FTIR spectroscopy was successfully used to confirm that the previously observed morphological differences between the inner and outer regions of the SC are reflected in variations in permeability. This heterogeneity contrasts with the normal assumption that the SC is of homoge-

neous resistivity. Although the model used to generate this data necessarily assumed homogeneity of the SC, and hence is somewhat inappropriate, the nature of the observed differences does indicate that real variation in permeability exists.

It was also shown that diffusional parameters obtained using in-vitro ATR-FTIR spectroscopy showed very good agreement with those obtained by other workers in-vivo. The combination of diffusion cell data and ATR-FTIR spectroscopic data was also used to determine diffusional pathlengths. In three synthetic silicone membranes of varying thickness, diffusional pathlengths were shown to be similar to their overall thickness. For reasons unknown, the degree of correlation appeared to improve with the thinner membranes (99.7% for a membrane of 90 μm thickness). For human SC, where the diffusional route has previously been thought to be a lengthy and tortuous pathway through the intercellular lipids and around the corneocytes (Potts and Francoeur, 1991; Albery and Hadgraft, 1979), the diffusional pathlength was found to be similar to its thickness. SC integrity was not compromised by the preparative procedures, as demonstrated by monitoring the diffusion of tritiated water across full-thickness, epidermal, and SC membranes. During all stages of the experiments the SC was fully hydrated by soaking in aqueous media, and from previous publications (Bouwstra et al., 1991; van Hal et al., 1996), it is clear that water penetrates cellular and intercellular regions of the SC. Therefore, it is possible that its presence may produce a change in diffusional pathlength, and a direct route across the swollen corneocytes may exist. Alternatively, as the apparent pathlength is a reflection of total length of rate limiting steps in a diffusional process rather than overall diffusional distance, it may imply that, in fully hydrated SC, molecular lateral diffusion within lipid bilayers is a relatively rapid process.

These conclusions should be borne in mind in the interpretation of barrier resistance measurements, and also in the design of in vitro and in vivo permeation experiments and the interpretation of their data.

**Acknowledgements**

The authors would like to thank the EPSRC for supporting this project.

## Appendix A. Prediction of the relationship between depth of IR beam penetration into stratum corneum and structural density

The outer layers of the SC are known to be less dense than the deeper layers. The refractive index, $n_r$, of a substance is defined by the ratio of the velocity of light in that substance, $v$, to the velocity of light in a vacuum, $c$, (Eq. (A1)).

$$n_r = \frac{c}{v} \tag{A1}$$

Refractive indices are always greater than 1.0 implying that the velocity of light is lower in more dense material and that therefore as density increases the refractive index will be raised. Eq. (A2) shows the exponential decay relationship between the energy, $E(c)$ of the IR wave entering a substance placed on an ATR crystal and the initial energy of the wave at the interface, $E_0$. The parameter $\gamma$ is defined as the depth constant which is a reflection of the rapidity of signal decay. The value of $\gamma$ is related to a number of physical parameters that are system dependent as shown in Eq. (A3) where, $n_c$ is the refractive index of the crystal, $n_s$ is the refractive index of the skin, $\chi$ is the wavelength of the light and $\theta$ is the angle of incidence.

$$E(\chi) = E_0 \exp[-\gamma.\chi] \tag{A2}$$

$$\gamma = \frac{2\pi n_c}{\lambda}\left[\sin^2\theta - \left(\frac{n_s}{n_c}\right)^2\right]^{0.5} \tag{A3}$$

Using Eq. (A2) and Eq. (A3), we can examine the effect of increasing the density of the skin on the depth of penetration of the beam into it. The following parameters are fixed for the system used in this work; $\chi = 4.483$ μm (2230 $cm^{-1}$ being the wavenumber at which the CN group absorbs), $n_c = 2.43$ (from manufacturers specifications), $\theta = 45°$ (defined by the cut of the ATR crystal used in the work), $E_0$ (the IR beam intensity at the crys-

tal/membrane interface) was set as unity. Using these values in Eq. (A2) and Eq. (A3) we can model the effect of changing $n_s$ (the refractive index of the SC) on the decay profile of the IR evanescent wave within the SC. This decay profile is the determining factor in the effective penetration depth of the IR beam into the SC, and upon reduction of $n_s$ from 1.8 to 1.0 (arbitrarily chosen values) this model predicted a reduced depth of penetration. Hence, a lower SC refractive index implies a lower penetration depth and resultant signal. The inner layers of the SC are more dense than the outer layers. If the velocity of light is lower in a more dense medium then it will be lower in the inner SC than the outer SC. Hence, the refractive index of the inner layers will be greater than that of the outer layers and the IR beam will penetrate the inner layers to a greater depth than the outer layers.

## References


Albery, W.J., Hadgraft, J., 1979. Percutaneous absorption: In vivo experiments. J. Pharm. Pharmacol. 31, 140–147.

Bouwstra, J.A., Gooris, G.S., van der Spek, J., Bras, W., 1991. Structural investigations of human stratum corneum by small angle X-ray scattering. J. Invest. Dermatol. 97, 1005–1012.

Elias, P.M., 1991. Epidermal barrier function: intercellular lamellar lipid structures, origin, composition and metabolism. J. Control. Rel. 15, 199–208.

Farinas, K.C., Doh, L., Venkatraman, S., Potts, R.O., 1994. Characterisation of solute diffusion in a polymer using ATR-FTIR spectroscopy and bulk transport techniques. Macromolecules 27, 5220–5222.

Harrick, N.J., 1967. Internal Reflection Spectroscopy. Wiley, New York.

Harrison, J.E., Watkinson, A.C., Green, D.M., Hadgraft, J., Brain, K.R., 1996. The relative effect of Azone and Transcutol on permeant diffusivity and solubility in human stratum corneum. Pharm. Res. 13, 542–546.

Knutson, K., Potts, R.O., Guzek, D.B., Golden, G.M., McKie, J.E., Lambert, W.J., Higuchi, W.I., 1985. Macro- and molecular physicalchemical considerations in understanding drug transport in the stratum corneum. J. Control. Rel. 2, 67–87.

Pellett, M.A., Watkinson, A.C., Brain, K.R., Hadgraft, J., 1995. An investigation into the validity of deuterated labelling of compounds in relation to their diffusion within synthetic membranes. In: Kellaway, I.W., Hadgraft, J. (Eds.), Proc. 4th UKaps Annual Conference; STS Publishing, Cardiff, pp. 68.

Pellett, M.A., Watkinson, A.C., Hadgraft, J., Brain, K.R., 1997. Comparison of permeability data from traditional diffusion cells and ATR-FTIR spectroscopy. Part I. Synthetic Membranes. Int. J. Pharm. 154, 205–215.

Pirot, F., Kalia, Y.N., Stinchcomb, A.L., Bunge, A., Guy, R.H., 1997. Characterisation of the permeability barrier of human skin in-vitro. Proc. Nat. Acad. Sci. 94, 1562–1567.

Potts, R.O., Francoeur, M.L., 1991. The influence of stratum corneum morphology on water permeability. J. Invest. Dermatol. 96, 495–499.

Potts, R.O., Guy, R.H., 1994. Drug transport across the stratum corneum and the attainment of steady-state flux. In: Proceedings of the 21st International Symposium on Controlled Release of Bioactive Materials (Nice); Controlled Release Society, Deerfield, USA, pp. 162–163.

Roberts, M.S., Walker, M., 1993. Water the most natural penetration enhancer. In: Walters, K.A., Hadgraft, J. (Eds.), Pharmaceutical Skin Penetration Enhancement, Marcel Dekker, New York, pp. 1–30.

van Hal, D.A., Jeremiasse, E., Junginger, H.E., Spies, F., Bouwstra, J.A., 1996. Structure of fully hydrated human stratum corneum-a freeze fracture electron microscopy study. J. Invest. Dermatol. 106, 89–95.

Watkinson, A.C., Bunge, A.L., Hadgraft, J., Naik, A., 1992. Computer simulation of stratum corneum concentration depth profiles. Int. J. Pharm. 87, 175–182.

Watkinson, A.C., Hadgraft, J., Walters, K.A., Brain, K.R., 1994. Skin penetration of cosmetic ingredients-predictive methods and risk assessment. In: Proceedings of the 18th International IFSCC congress, Venice, pp. 889–901.

Watkinson, A.C., Joubin, H., Green, D.M., Brain, K.R., Hadgraft, J., 1995. The influence of vehicle on permeation from saturated solutions. Int. J. Pharm. 121, 27–36.

Wurster, D.E., Buraphacheep, V., Patel, J.M., 1993. The determination of the diffusion coefficient in semi solids by Fourier transfrom (FTIR) spectroscopy. Pharm. Res. 10, 616–620.